Nuclear Physics A391 (1982) 221–236

HIGH-SPIN STATES IN ^{218}Ra

J. FERNÁNDEZ-NIELLO †, H. PUCHTA, F. RIESS and W. TRAUTMANN

Sektion Physik, Universität München, D-8046 Garching, FR Germany

Received 28 May 1982

Abstract: Yrast states in ^{218}Ra up to spin and parity $I^\pi = 17^-$ were identified by means of the ^{208}Pb(^{13}C, 3n) reaction and standard γ-ray spectroscopic techniques. The level scheme is characterized by two bands of opposite parity with nearly constant level spacing. A cascade of strong E1 interband transitions connects both bands.

The results are discussed within the systematics of the even Ra isotopes. The negative-parity band which is observed from the $I^\pi = 5^-$ to the $I^\pi = 17^-$ state, is interpreted as an octupole vibrational band. The level scheme can be well reproduced in the vibrational limit of the interacting boson approximation (IBA1) which fails, however, to explain the strong E1 feeding of the negative-parity band from the ground-state band

E NUCLEAR REACTIONS ^{208}Pb(^{13}C, 3nγ), E = 60–83 MeV; measured E_γ, $I_\gamma(E,t)$, $I_\gamma(\theta,t)$, linear polarization P_γ, $\gamma\gamma$-, γX-ray-coin. ^{218}Ra deduced level energies J, π, B(E1)/B(E2) ratios. Planar Ge, Ge(Li), NaI(Tl) detectors, five-detector Compton polarimeter, enriched targets, pulsed beam.

1. Introduction

The radium isotopes have been investigated over a large isotopic range, starting from spherical shell-model nuclei and extending into the deformed region near the valley of quasi-stability. Neutron deficient ^{214}Ra, at the $N = 126$ neutron shell closure, and ^{216}Ra have been studied via (HI, xn) reactions [1–3]). High-spin isomers were found in these nuclei, and their structure is understood on the basis of the spherical shell model. In heavier isotopes ($A \geq 220$), nuclear structure information relies on α- and β-decay studies [4]) with the exception of ^{226}Ra where high-spin states up to $I^\pi = 12^+$ were populated by Coulomb excitation [5]). Here collective features prevail.

Until now, only scarce information has been available about the transitional region ($216 < A \leq 220$), limited to a few excited states in ^{217,220}Ra which were identified in α-decay experiments [4]). On the other hand, these nuclei are of considerable interest since here the gradual onset of collectivity may be studied as more and more neutrons are added outside the $N = 126$ shell. Of particular interest are the negative-parity states

† On leave from Comisión Nacional de Energía Atómica, Buenos Aires, Argentina.

which in ^{214,216}Ra were seen only above the $I^{\pi} = 11^{-}$ proton $h_{9/2}i_{13/2}$ intruder state [1,3]). The nature of the 1^{-}, 3^{-} and 5^{-} states, identified in even isotopes with $A \geqq 220$ [refs. [5-8])], however, is still being discussed, although an octupole vibrational origin is strongly favored in a recent analysis [9]) of existing data.

It is our aim to fill in the existing gap by studying these nuclei in the transition region. The present paper reports the results obtained for ^{218}Ra, populated via the ^{208}Pb(^{13}C, 3n) reaction. No excited states were previously known in this nucleus. The measurements are described and illustrated in sect. 2. The deduced level scheme and the experimental evidence supporting it are given in sect. 3. In sect. 4, the structure of ^{218}Ra is compared to the phenomenological systematics of even Ra isotopes and discussed in the framework of the interacting boson approximation [10]).

2. Measurements

Excited states in ^{218}Ra were populated by means of the ^{208}Pb(^{13}C, 3n) reaction. Isotopically enriched (97 %) self-supporting targets of 1 to 1.3 mg/cm^2 thickness were bombarded with ^{13}C beams, provided by the Munich MP Tandem Van de Graaff accelerator, at energies between 60 MeV and 83 MeV. The beam was stopped about 4 m behind the target in a concrete-shielded Faraday cup.

Gamma rays were assigned to ^{218}Ra on the basis of excitation functions and γ-X-ray coincidences. Gamma-gamma coincidence data and the results of angular distribution and linear polarization measurements served to build up the level scheme and to determine spins and parities. In the following, these experiments are described in more detail.

2.1. EXCITATION FUNCTIONS

Excitation functions were measured with pulsed beams (FWHM $\approx$ 1.5 ns) in the energy range between 60 MeV and 83 MeV. Gamma rays were detected in a Ge(Li) detector (11 % efficiency) and a planar Ge detector (10 cm^3 volume), both placed 20 cm from the target and at $\pm 90°$ with respect to the beam axis. Prompt and delayed spectra were accumulated both in singles mode and, in order to suppress low multiplicity events, gated by coincident γ-rays detected in a 12.7 cm $\times$ 12.7 cm NaI detector. The spectra were normalized according to the integrated beam current.

In-beam γ-ray spectra, measured at bombarding energies of 65 MeV, 74 MeV and 83 MeV with the Ge(Li) detector gated by the NaI detector, are shown in fig. 1. The observed γ-rays fall into three groups (figs. 1, 2). The first group which contains the known transitions in ^{216}Ra [refs. [2,3])] appears at bombarding energies exceeding 74 MeV (5n channel). The second group, including two transitions between known levels in ^{217}Ra [ref. [11])], has its maximum intensity at a bombarding energy near 77 MeV (4n channel). Hence, the third group, peaking at 67 MeV, was associated with the 3n

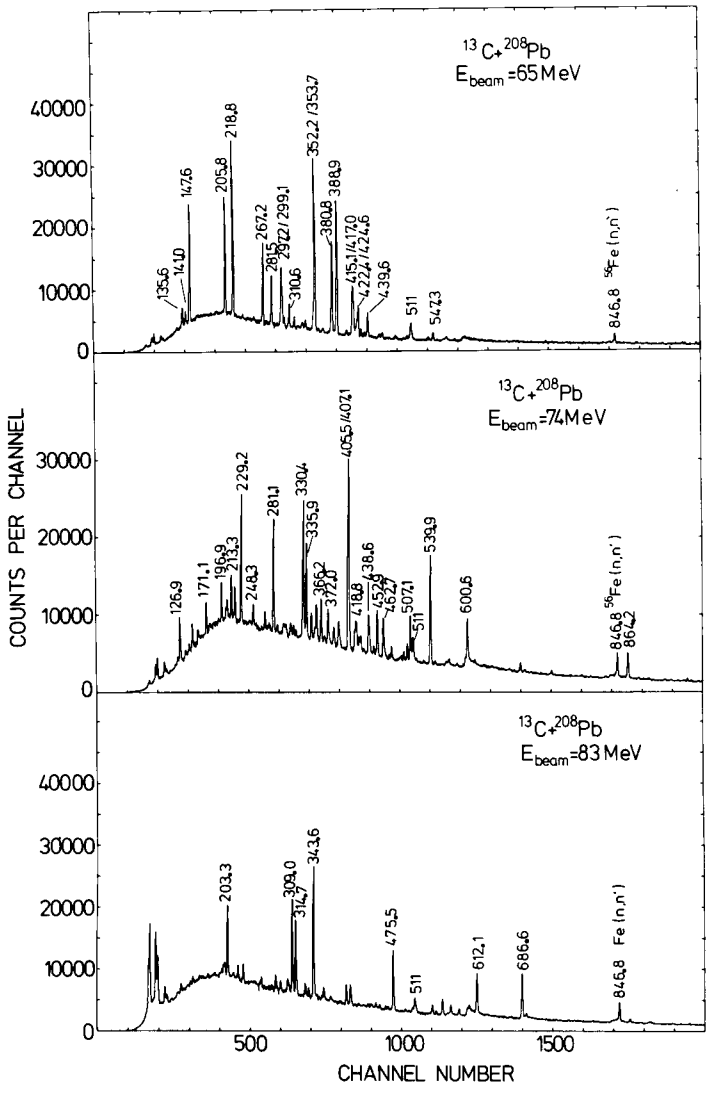

Fig. 1. In-beam γ-ray spectra measured with a Ge(Li) detector in coincidence with a 5″ × 5″ NaI detector following the reaction $^{208}Pb(^{13}C, xn)$ at E = 65 MeV, 74 MeV and 83 MeV. Gamma-ray lines from transitions in ^{218}Ra (65 MeV), ^{217}Ra (74 MeV) and ^{216}Ra (83 MeV) are labeled.

channel leading to ^{218}Ra. The Z = 88 assignment was confirmed by the measurement of γ-X-ray coincidences (subsect. 2.2).

For γ-rays measured with the planar detector the time with respect to the arrival of the beam burst was recorded with a resolution of 2.5 ns (FWHM). However, no isomeric transitions in ^{218}Ra with lifetimes exceeding that value were found.

Fission of the highly excited Ra nuclei did not appear as a strongly competing

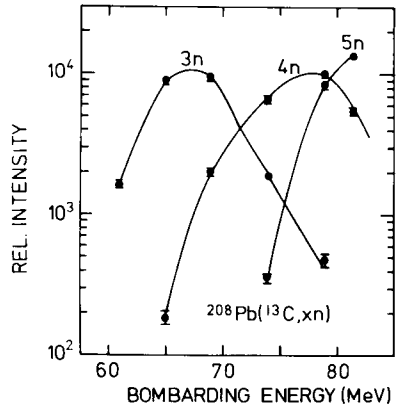

Fig. 2. Excitation functions for the most prominent γ-ray lines from excited ^{218}Ra (389 keV), ^{217}Ra (330 keV) and ^{216}Ra (688 keV) which show the relative strengths of the 3n, 4n and 5n channels of the ^{208}Pb(^{13}C, xn) reaction.

channel even at the highest bombarding energy. This was expected since the fission barrier should exceed 8 MeV in the whole spin range covered by this reaction [12]).

2.2. COINCIDENCE MEASUREMENTS

Gamma-gamma and γ-X-ray coincidences were measured at a bombarding energy of 69 MeV, i.e. 2 MeV higher than the optimum energy of the 3n channel, in order to enhance the population of high-spin states in ^{218}Ra. At this energy, ^{217}Ra is produced with an intensity of 40 % of that of ^{218}Ra.

A coincidence was required between a true coaxial Ge(Li) detector (efficiency 24 %), positioned at 90° with respect to the beam axis, and either a second Ge(Li) detector of equal size at 145° or a planar Ge detector (volume 10 cm^3) at 25°. In addition, an array of two 10.2 cm × 10.2 cm and one 12.7 cm × 12.7 cm NaI detectors was set up and, for each event, the number of detectors which had simultaneously fired was recorded. The comparison of coincidence spectra gated by different numbers of NaI events, i.e. by different multiplicity requirements, did not reveal significant differences in the relative intensities of the observed γ-ray lines. This implies that contributions from activities, which are expected to have low multiplicities, are small.

The analysis of the X-ray spectrum, measured with the planar detector in coincidence with the Ge(Li) detector, proved that at this bombarding energy the neutron evaporation channels dominate and that αxn reactions, leading to Rn isotopes, are about two orders of magnitude less intense (fig. 3).

2.3. ANGULAR DISTRIBUTIONS

Angular distributions were measured with beams of 65 MeV and 69 MeV energy.

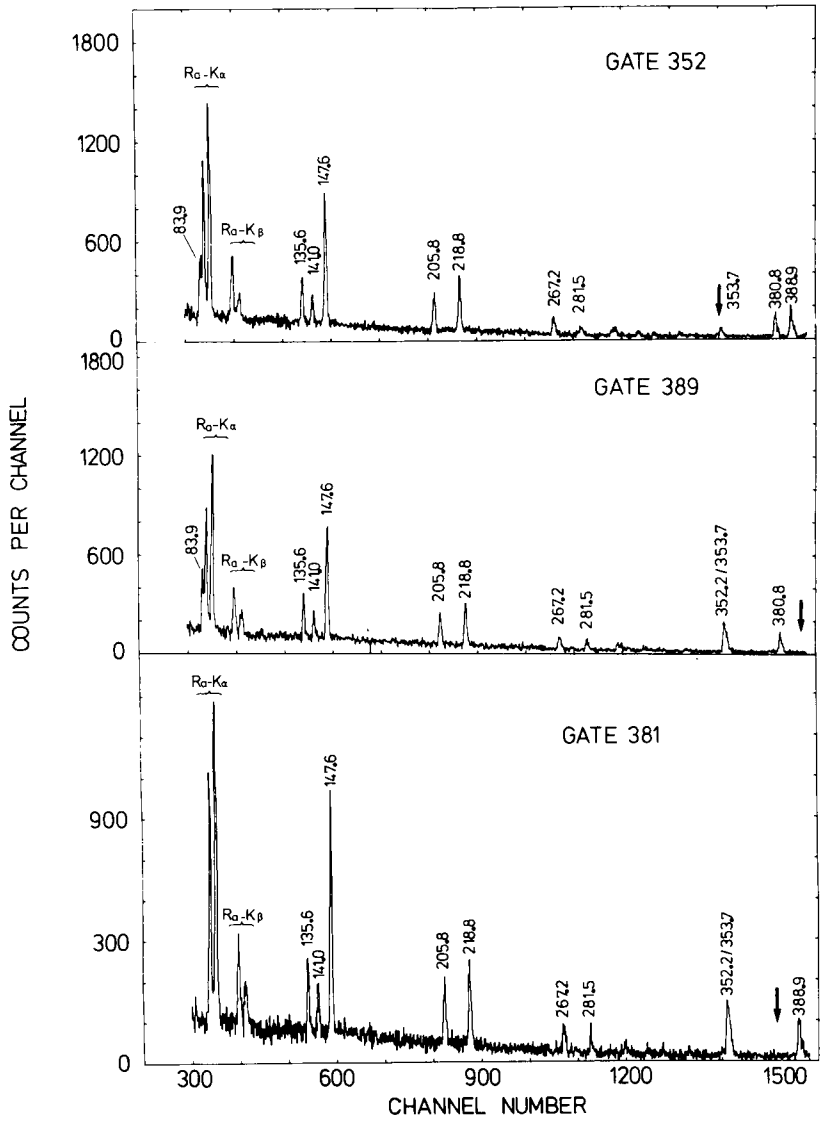

Fig. 3. Gamma-ray spectra measured with the planar Ge detector in coincidence with a Ge(Li) detector. The arrows indicate the position of the gating lines. Note the Ra X-rays and the 84 keV γ-ray which is absent in the "gate 381" spectrum.

Gamma-ray spectra were measured at angles between 30° and 90° with a true-coaxial Ge(Li) detector of 24 % efficiency, placed at a distance of 20 cm from the target. The normalization was based on spectra measured with a second Ge(Li) detector held at a fixed position.

The A_2 and A_4 coefficients, deduced from a fit of the normalized intensities to a

TABLE 1

Spectroscopic data of γ-transitions in ^{218}Ra

E_γ	I [a])	A_2	A_4	P_γ	Type
83.9(3)	25(5)				E1 [b])
135.6(2)	28(3)	−0.22(14)	0.14(19)	0.37(12)	E1
141.0(3)	17(2)	−0.31(12)	0.12(14)	0.31(14)	E1
147.6(3) [c])	88(4)	−0.33(4)	−0.06(7)	0.27(5)	E1
205.8(2)	49(2)	−0.25(8)	0.02(5)	0.26(4)	E1
218.8(1)	75(3)	−0.21(5)	0.04(4)	0.26(3)	E1
267.2(2)	35(2)	−0.32(4)	−0.00(6)	0.28(5)	E1
281.5(2)	28(3)	−0.30(6)	−0.05(7)	0.29(5)	E1
297.2(2)	29(2)	−0.37(3)	0.04(4)	0.22(4)	E1
299.1(3)	18(3)	−0.17(5)	0.05(7)		E1
303.0(3)	5(1)	0.26(7)	−0.12(9)		E2
310.6(3)	13(2)	−0.67(7)	−0.06(8)	−0.24(12)	M1/E2
332.1(3)	10(2)				
352.2(1)	100(5)	0.24(2)	−0.09(3)	0.35(4)	E2
353.7(2)	28(4)				E2
380.8(2)	71(3)	0.24(3)	−0.08(4)	0.39(8)	E2
388.9(1)	100(2)	0.23(3)	−0.08(4)	0.34(8)	E2
415.1(2) [c])	50(2)	0.13(7)	−0.09(8)	0.44(8)	E2
417.0(3)	37(3)	0.36(9)	−0.20(10)		E2
422.4(2)	34(2)	0.26(1)	−0.10(9)	0.40(9)	E2
424.6(2)	17(2)	0.11(6)	−0.15(9)		E2
429.5(3)	8(1)	0.20(7)	−0.05(8)	0.46(21)	E2
434.9(3)	6(1)	0.22(8)	0.04(7)	0.44(28)	E2
439.6(2)	26(2)	0.14(4)	0.08(11)	0.38(11)	E2
547.3(3)	15(1)	0.39(8)	0.05(8)	0.44(8)	E2

[a]) Corrected for internal conversion.
[b]) M1 or E2 character would lead to unreasonably high intensities for this line.
[c]) Unresolved doublets.

Legendre polynomial expansion, are listed in table 1. They indicate either pure dipole or pure quadrupole nature for transitions in ^{218}Ra. The measured angular distributions compare well with the predictions [13]) for stretched cascades starting from an initial state with spin $I = 20$ and a gaussian substate distribution centered at $M = 0$ with a standard deviation $\sigma = 2.0$. (The large width may be partly due to hyperfine interactions.) The angular distributions of the most prominent lines are shown in fig. 4.

2.4. LINEAR POLARIZATION

The linear polarization P_γ was measured with a Compton polarimeter built from five γ-ray detectors. Its design represents a natural extension of commonly used three-detector polarimeters [14]) with the advantage of a detection efficiency twice as high. In

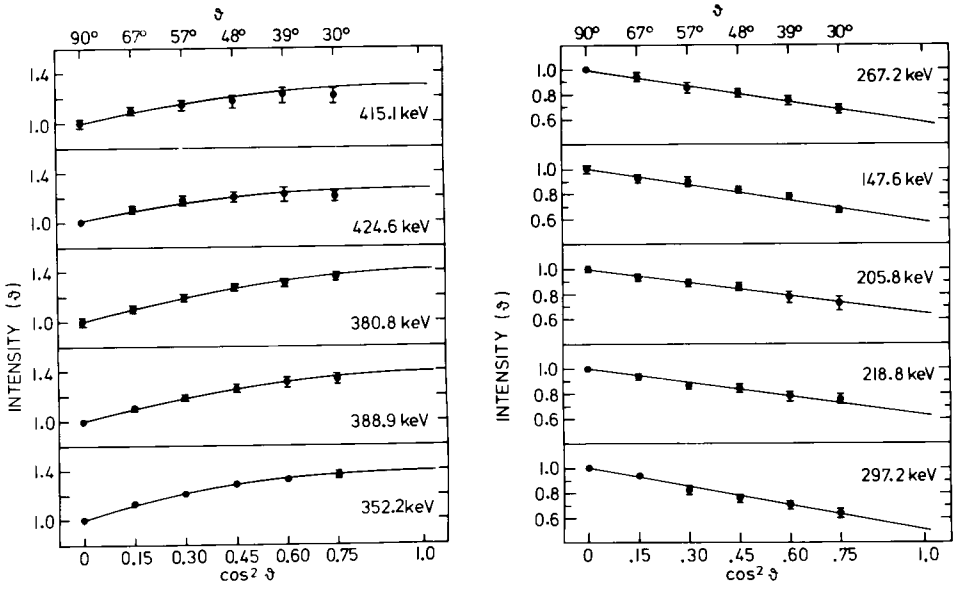

Fig. 4. Measured angular distributions of prominent dipole and quadrupole transitions in ^{218}Ra. The full lines represent the results of calculations (see text).

order to enhance the efficiency at low γ-ray energies, a planar Ge detector (36 cm^3 volume) was used as the central scatterer. It was surrounded by four nearly identical true-coaxial detectors (each of 24 % efficiency) placed up and down and left and right from the scatterer. The scatterer was positioned at 90° with respect to the beam axis and 21 cm from the target. The absorber detectors were shielded from the primary radiation by lead of 10 cm thickness.

The detection efficiencies of the four scatterer-absorber detector combinations were measured with γ-ray sources placed in the target position. The polarization sensitivity $Q(E_\gamma)$ was calibrated in-beam with the three strongest lines of the ground-state band of ^{218}Ra(E_γ = 352, 389 and 381 keV) and extrapolated over the range of interest by assuming it to be a constant fraction of Q_{KN}, the sensitivity predicted by the Klein-Nishina formula for a scattering angle $\xi = 90°$ and point detectors [14]). The fairly large value of

$$Q(E_\gamma) = (0.83 \pm 0.03) Q_{KN}$$

is a consequence of the application of appropriate cosξ gates [14]) during playback of the data.

With this setup it was possible to determine the linear polarization of most of the γ-rays from ^{218}Ra, including the low-lying dipole transitions, with energies $E_\gamma \geqq 136$ keV. The results confirmed the E2 nature of the quadrupole transitions and proved all

dipole transitions to be E1, except for the $E_\gamma = 311$ keV line which is most probably of mixed M1/E2 character. A summary of the spectroscopic information on γ-rays assigned to ^{218}Ra is given in table 1.

3. The level scheme of ^{218}Ra

For the γ-ray ordering, the relative intensities of transitions in ^{218}Ra and the excitation functions were used. In particular, the excitation functions measured in 1 MeV steps from 60 MeV near threshold to higher energies (fig. 5) proved to be very

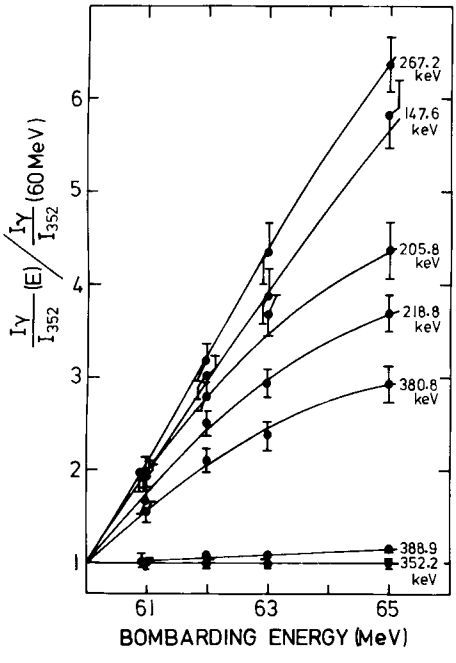

Fig. 5. Excitation functions of several transitions in ^{218}Ra relative to the 352 keV transition and normalized to the respective values at $E = 60$ MeV.

helpful since the maximum spin input increases rapidly over this energy range. [The Bass model [15]) predicts a fusion threshold of $E_{th} = 61$ MeV and a maximum spin $l_{max} = 16$ at $E = 65$ MeV.] A hint to the structure of the level scheme was found in the fact that the energies of several E2 transitions equal the sum of the energies of two E1 transitions (table 1). On the other hand, the situation was complicated by the occurrence of transitions close in energy and of two unresolved doublets. Arguments derived from the requirement of a monotonically increasing intensity flow along the yrast line were used in some cases. The deduced level scheme is presented in fig. 6, the experimental evidence supporting it will be discussed in the following.

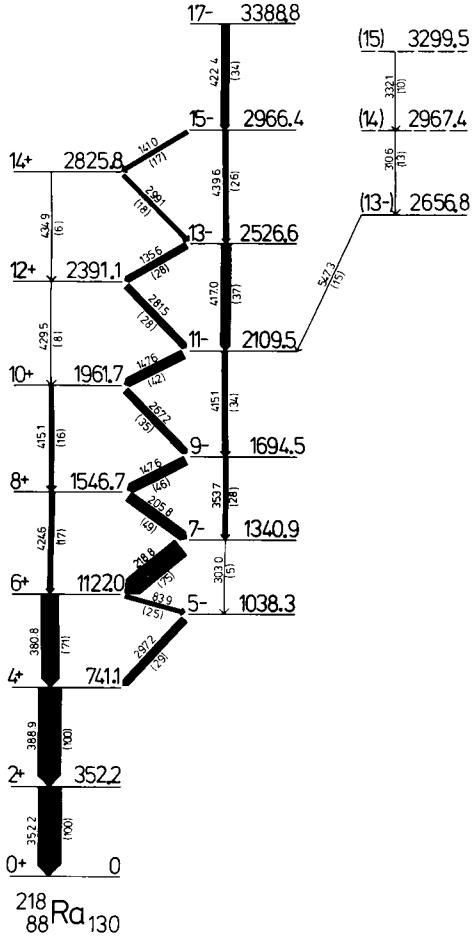

Fig. 6. Level scheme of ^{218}Ra established in this work. The excitation energies were calculated by a weighted addition of the transition energies. The intensities are normalized to I (352 keV) = 100.

The 2^+, 4^+ and 6^+ states. The sequence of the three strongest E2 transitions, leading from $I^\pi = 6^+$ to the ground state, was determined from the excitation functions (fig. 5). The identity of the $6^+ \rightarrow 4^+$ transition is also apparent from the relative intensities at $E = 69$ MeV (fig. 6) whereas the strengths of the 352 keV and 389 keV lines are nearly equal over the whole energy range. The strengths of the former hne were obtained from fits to the unresolved line-shapes of the 352 keV and 354 keV transitions, keeping the peak energies at fixed values. The double ratio of intensities

$$\frac{I_{389}}{I_{352}}(65\ \text{MeV}) \Big/ \frac{I_{389}}{I_{352}}(60\ \text{MeV}) = 1.17 \pm 0.03$$

led us to associate the 352 keV line with the $2^+ \rightarrow 0^+$ transition.

The 5⁻ state. This is the lowest observed state of a negative-parity band. The parity assignment is based on the electric character of the interband dipole transitions and the E2 character of the intraband transitions. The 84 keV transition, feeding the 5^- state from the 6^+ member of the ground-state band, was identified in coincidence spectra measured with the planar Ge detector and, by setting appropriate gates, was found to bypass the 381 keV transition (fig. 3).

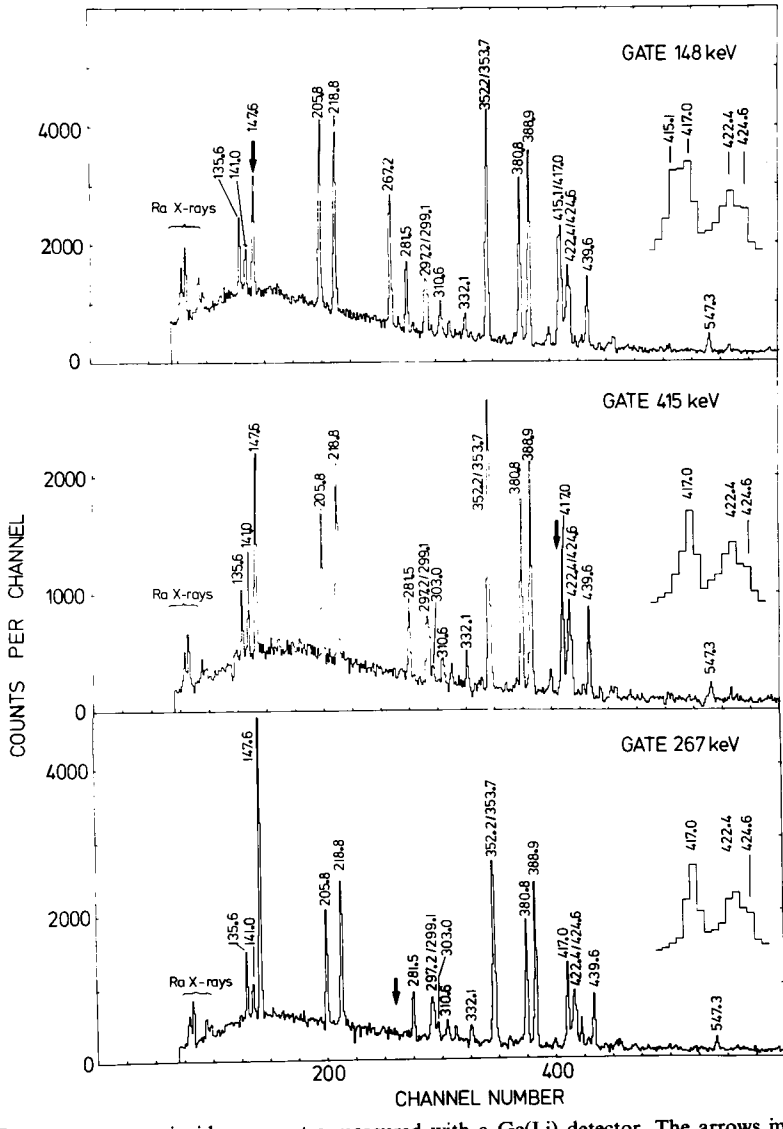

Fig. 7. Gamma-gamma coincidence spectra measured with a Ge(Li) detector. The arrows indicate the position of the gating lines. The insets show the region near 420 keV on an expanded scale.

The 148 keV doublet. The two transitions with this energy appear in true coincidence (fig. 7). From the line widths and peak positions found in various spectra measured with the planar detector [resolution of 690 eV (FWHM) at 122 keV] in singles and coincidence mode we estimate that the two lines differ by less than 300 eV in energy (3 standard deviations). Their location in the level scheme is supported by the observation that the intensity of the 148 keV line is reduced in the spectra gated by the 354 keV and 429 keV transitions.

The 415 keV doublet. This doublet does not appear in true coincidence (fig. 7). However, the existence of the 148 keV doublet at the assigned positions of the E1 cascade requires the paralleling E2 transitions to have the same energy. This is confirmed by the spectra gated with the 354 keV and 429 keV transitions and by the agreement of the measured and expected intensity patterns.

The 267 keV dipole transition was the only other line which did not appear in coincidence with the 415 keV doublet (fig. 7) and was therefore placed parallel to it.

Yrast states at $E_x > 2$ MeV. The level sequence of the positive- and negative-parity bands in the region above the doublets is uniquely determined by the coincidence data. The two bands could be followed up to spins of 14 and 17, respectively. No candidates for higher-lying transitions appeared in the spectra.

The third band. Three members of a third band, feeding into the negative-parity band at the 11^- level, were found. The 547 keV interband transition is most probably E2, and the 311 keV transition most probably of mixed M1/E2 character (table 1).

4. Discussion

The level scheme of ^{218}Ra is characterized by the existence of two bands of opposite parity and nearly equidistant level spacing. They are strongly connected by an E1 cascade. In particular, the strong feeding of the negative-parity band from members of

TABLE 2

B(E1)/B(E2) branching ratios for the deexcitation of levels in ^{218}Ra

Level energy (keV)	I^π	$B(E1)/B(E2)$ (10^{-6} fm^{-2})
1122	6^+	3.7 ± 0.8
1341	7^-	2.8 ± 0.6
1547	8^+	3.5 ± 0.4
1694	9^-	2.2 ± 0.4
1962	10^+	1.1 ± 0.2
2109	11^-	3.6 ± 0.4
2391	12^+	1.8 ± 0.3
2527	13^-	2.9 ± 0.4
2826	14^+	1.3 ± 0.3
2966	15^-	2.9 ± 0.4

the ground-state band is rather striking. Another interesting feature, deduced from the level scheme, concerns the $B(E1)/B(E2)$ branching ratios. We find that their values are the same within a factor of 3 to 4, independent of spin and parity of the decaying state (table 2). In the following subsections we compare the properties of ^{218}Ra to those of the neighbouring even Ra isotopes and to IBA predictions.

4.1. THE POSITIVE-PARITY BAND

The positive-parity band fits well into the systematics of the even Ra isotopes (fig. 8). The monotonic decrease in energy of the 2^+ excitation and higher states illustrates the

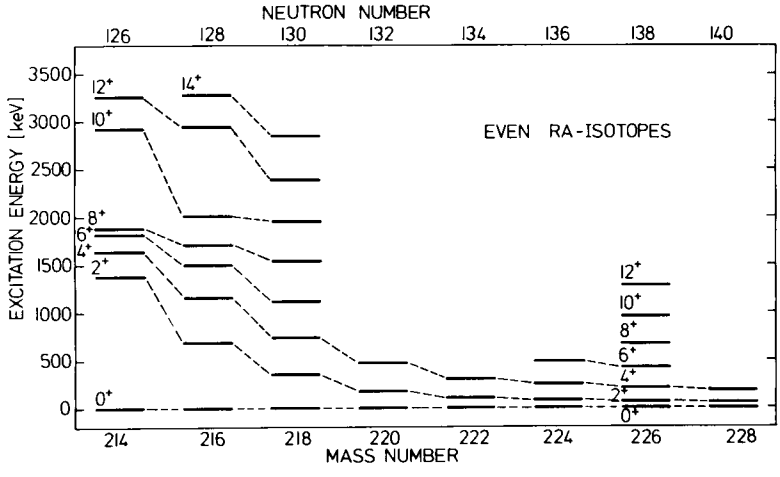

Fig. 8. Positive-parity states in even Ra nuclei. The data are from refs. [1-7]) and this work.

gradual increase in collectivity as more neutrons are added to the $N = 126$ closed shell. The transitional character of ^{218}Ra is obvious. It links the lighter isotopes where single-particle structure dominates to the heavier nuclei with rotational behavior. The almost equidistant level spacing suggests a vibrational structure and a nearly spherical shape for ^{218}Ra. Sphericity ($|\beta| < 0.01$) is also expected from calculations of ground-state properties based on the Strutinsky method [16]).

On the other hand, the irregularities in the level spacing may only be properly accounted for by a shell-model calculation. Level sequencies of similar type also exist in transitional rare-earth nuclei, as e.g. in ^{156}Yb [ref. [17])], which has 6 protons and 4 neutrons outside the $Z = 64$, $N = 82$ core and, in that respect, might be considered analogous to ^{218}Ra. Although absolute strengths of transitions in ^{218}Ra have not been determined in this work it is possible to obtain an estimate of the collectivity of the $2^+ \rightarrow 0^+$ transition by applying the empirical rule of Grodzins [18]). It yields a strength of ≈ 30 single-particle units, suggesting that many configurations are admixed into

these states and that both proton $(h_{\frac{9}{2}})^6$ and neutron $(g_{\frac{9}{2}})^4$ configurations contribute. It should be interesting to see if shell-model calculations based on effective two-nucleon interactions which can account for the structure of ^{216}Ra [ref. [3])] can be applied to this case.

4.2. THE NEGATIVE-PARITY BAND

The negative-parity states form a band with similar energy spacings as the ground-state band. The lowest observed state has $I^\pi = 5^-$ since band members with smaller spins (probably $I^\pi = 1^-, 3^-$) are not populated in this reaction. An extrapolation from the known states of this band yields values between 600 keV and 800 keV for their excitation energies and explains why they are bypassed by the intensity flow (cf. fig. 6).

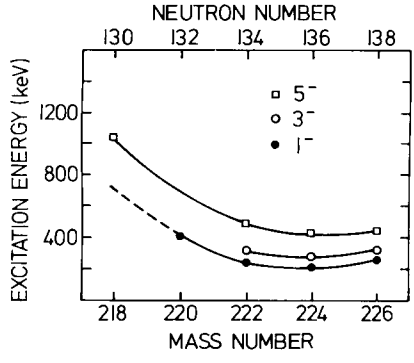

Fig. 9. Low-lying negative-parity states in even Ra nuclei. The data are from refs. [4-7]) and this work. A smooth extrapolation from the known 1^- states (dashed line) coincides with the level of excitation where the low-spin members of the negative-parity band are expected in ^{218}Ra (cf. fig. 6).

A comparison of the 5^- excitation energy with the systematics of known negative-parity states in heavier Ra isotopes (fig. 9) points to a similar nature of all these states. Up to now, however, the structure of the low-lying negative-parity states in $A \geqq 220$ Ra nuclei has been a matter of discussion. Following arguments given by Peker *et al.* [9]) an octupole vibrational origin seems most probable although the respective two-phonon octupole states with $I^\pi = 0^+$ were not observed in α-decay experiments [6,7]). An alternative explanation by Möller *et al.* [19]) assumes that $K^\pi = 0^+$ and $K^\pi = 0^-$ states belong to different minima in the potential energy surface. They suggest a stable octupole deformation for the negative-parity states. In this case, transitions feeding or depopulating this band should be strongly hindered since they involve a nuclear shape change. However, such hindrance is not observed in $A \geqq 220$ Ra nuclei [ref. [9]) and references therein].

Similarly, we do not observe retardation of these transitions in ^{218}Ra. The B(E1)/B(E2) branching ratios (table 2) and the estimate of B(E2) $\approx$ 30 Weisskopf units

(W.u.) for the E2 intraband transitions (see above) yield a strength of $B(\mathrm{E1}) \approx 10^{-3}$ W.u. An E1 hindrance of this order can certainly be considered typical in this mass region [20]) and does not imply any additional retardation. Moreover, the remarkable fact that nearly identical branching ratios were found for the deexcitation of positive- *and* negative-parity states suggests that the vibrational-type structure of both bands is in fact of rather similar origin. We therefore conclude that the most probable explanation for the negative-parity band is that of an octupole vibrational band. We do not offer evidence for an 11^- state having the configuration $\pi(h_{\frac{9}{2}}, i_{\frac{13}{2}})$ which is seen as a low-lying isomeric state in ^{214,216}Ra and some of their Rn and Po isotones [1-4]). As in the rotational case discussed by Vogel [21]), the negative-parity band may assume a two-quasiparticle character at higher spins.

4.3. IBA PREDICTIONS

Guided by the collective features observed in ^{218}Ra and by the vibrational pattern of the two bands built on the ground state and the octupole vibrational excitation we have attempted to interpret our results in terms of the interacting boson approximation [IBA, ref. [10]); in the following the notation used in this reference will be adopted]. In the vibrational limit without cut-off, the energies $E_{\mathrm{g.s.b.}}$ of the ground-state band are given by

$$E_{\mathrm{g.s.b.}}(I = 2n_{\mathrm{d}}) = \varepsilon_{\mathrm{d}} n_{\mathrm{d}} + \tfrac{1}{2} c_4 n_{\mathrm{d}}(n_{\mathrm{d}} - 1),$$

where n_{d} represents the number of d-bosons ($L = 2$), ε_{d} their excitation energy and c_4 the coupling between them. The excitation of an f-boson ($L = 3$) and its coupling to the n_{d} d-bosons require two additional terms for the description of the octupole vibrational band (o.v.b.):

$$E_{\mathrm{o.v.b.}}(I = 2n_{\mathrm{d}} + 3) = E_{\mathrm{g.s.b.}}(2n_{\mathrm{d}}) + \varepsilon_{\mathrm{f}} + n_{\mathrm{d}} x_5.$$

Using these expressions we obtain an excellent fit to the experimental level scheme (fig. 10). The deduced parameters are $\varepsilon_{\mathrm{d}} = 361.2$ keV, $c_4 = 14.7$ keV, $\varepsilon_{\mathrm{s}} = 649.7$ keV and $x_5 = -15.1$ keV. In comparison with the fits to the level schemes of ^{150}Sm and ^{152}Gd which are characterized by similar d-boson excitation energies [10]) the small d-boson interaction term c_4 should be noted. The much smaller f-boson excitation energy is also expected from the point of view of shell-model considerations [22]).

In this limit of the IBA the branching ratios in the deexcitation of the negative-parity states can be expressed as [10]):

$$\frac{B(\mathrm{E1}, I = 2n_{\mathrm{d}} + 3 \to I' = 2n_{\mathrm{d}} + 2)}{B(\mathrm{E2}, I = 2n_{\mathrm{d}} + 3 \to I' = 2n_{\mathrm{d}} + 1)} = \frac{n_{\mathrm{d}} + 1}{7n_{\mathrm{d}}} C,$$

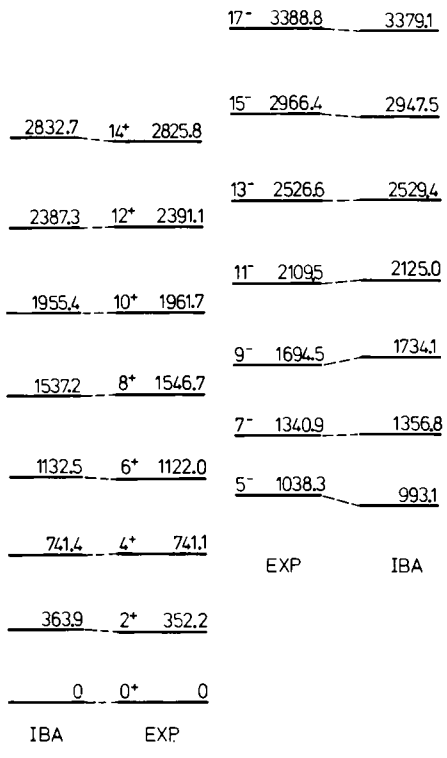

Fig. 10. Comparison of experimental level energies with IBA predictions (see text).

with C being a constant. In the case of ^{218}Ra we observe these branchings in the range of $7 \leqq I \leqq 15$, i.e. for $n_d \geqq 2$ where the formula predicts values nearly independent of I, in good agreement with experiment (table 2). However, within this limit of the IBA, the corresponding branching ratios for the members of the ground-state band should vanish since here the E1 transitions involve the simultaneous annihilation of two d-bosons. This is in striking contrast to experiment (table 2). Symmetry-breaking terms, treated as perturbation [10]), can also not account for the strong observed $B(E1)/B(E2)$ branching ratios of the members of the ground-state band. It therefore seems that in the case of ^{218}Ra the interacting boson approximation in the SU(5) limit cannot account for all experimentally observed data. It remains to be studied if other limits of the IBA [e.g. SU(3), ref. [23])] or an extension of the IBA to account for α-clustering which involves p-bosons [24]) may give a better account of the nature of the negative-parity band and the observed $B(E1)/B(E2)$ branching ratios.

5. Conclusion

The level scheme of ^{218}Ra, previously unknown, has been established up to spin $I^{\pi} = 17^{-}$. The excited levels group into two main bands of opposite parity and a third band of which only three levels were observed. The members of the two main bands are nearly evenly spaced in excitation energy, as characteristic of a vibrational behavior. The positive-parity band fits well into the systematics of even Ra isotopes and demonstrates the transitional character of ^{218}Ra. The negative-parity band is interpreted as an octupole vibrational band, as seen in heavier Ra nuclei. A strong E1 cascade connects both bands. The neraly constant $B(E1)/B(E2)$ branching ratiös suggest a rather similar structure of both bands. The vibrational limit of the interacting boson approximation yields a good description of the level scheme but fails to account for the E1 deexcitation of the members of the ground-state band.

We would like to thank Dr. H. Behrens and A. Lutz for their contributions during various stages of the experiment. Illuminating discussions with Prof. P. Ring are acknowledged. One of us (J.F.N.) is much indebted to Prof. J. de Boer for the warm hospitality and the excellent working conditions provided. He also gratefully acknowledges a grant from the Deutscher Akademischer Austauschdienst (DAAD). This work was supported by the Bundesministerium für Forschung und Technologie.

References

1) D. Horn, O. Häusser, B. Haas, T. K. Alexander, T. Faestermann, H. R. Andrews and D. Ward, Nucl. Phys. **A317** (1979) 520
2) T. Nomura, K. Hiruta, M. Yoshie, H. Ikezoe, T. Fukuda and O. Hashimoto, Phys. Lett. **58B** (1975) 273
3) T. Lönnroth, D. Horn, C. Baktash, C. J. Lister and G. R. Young, preprint 1981
4) Table of Isotopes, seventh edition, ed. C. M. Lederer and V. S. Shirley, (Wiley, New York, 1978)
5) R. Zimmermann, Thesis, Universität München (1980), unpublished
6) W. Kurcewicz, N. Kaffrell, N. Trautmann, A. Plochocki, J. Zylicz, K. Stryczniewicz and I. Yutlandov, Nucl. Phys. **A270** (1976) 175
7) W. Kurcewicz, N. Kaffrell, N. Trautmann, A. Plochocki, J. Zylicz, M. Matul and K. Stryczniewicz, Nucl. Phys. **A289** (1977) 1
8) F. S. Stephens, F. Asaro and I. Perlman, Phys. Rev. **107** (1957) 1091
9) L. K. Peker, J. H. Hamilton and J. O. Rasmussen, Phys. Rev. **C24** (1981) 1336
10) A. Arima and F. Iachello, Ann. of Phys. **99** (1976) 253
11) K. Valli, E. K. Hyde and J. Borggreen, Phys. Rev. **C1** (1970) 2115
12) C. G. Andersson, G. Hellström, G. Leander, I. Ragnarsson, S. Aberg, J. Krumlinde, S. G. Nilsson and Z. Szymański, Nucl. Phys. **A309** (1978) 141
13) K. S. Krane, R. M. Steffen and R. M. Wheeler, Nucl. Data Sect. **A11** (1973) 351
14) P. A. Butler, P. E. Carr, L. L. Gadeken, A. N. James, P. J. Nolan, J. F. Sharpey-Schafer, P. J. Twin and D. A. Viggars, Nucl. Instr. **108** (1973) 497
15) R. Bass, Phys. Lett **47B** (1973) 139
16) P. Möller, S. G. Nilsson and J. R. Nix, Nucl. Phys. **A229** (1974) 292
17) C. J. Lister, D. Horn, C. Baktash, E. der Mateosian, O. C. Kistner and A. W. Sunyar, Phys. Rev. **C23** (1981) 2078
18) L. Grodzins, Phys. Lett. **2** (1962) 88
19) P. Möller, S. G. Nilsson and R. K. Sheline, Phys. Lett. **40B** (1972) 329
20) C. F. Perdrisat, Rev. Mod. Phys. **38** (1966) 41
21) P. Vogel, Phys. Lett. **60B** (1976) 431
22) A. Bohr and B. R. Mottelson, Nuclear structure, vol. 2 (Benjamin, New York, 1975) p. 591
23) A. Arima and F. Iachello, Ann. of Phys. **111** (1978) 201
24) F. Iachello and A. D. Jackson, Phys. Lett. **108B** (1982) 151